

Turbulence closure in the light of phase transition

Mohammed A. Azim

Department of Mechanical Engineering, Bangladesh University of Engineering and Technology, Dhaka-1000, Bangladesh, email: azim@me.buet.ac.bd

In the present study, new turbulence closure equations are derived in the light of continuous (often termed second-order) phase transition. Closed form Reynolds averaged Navier-Stokes equations due to those closure equations are solved numerically for a plane turbulent free jet. Here, turbulent viscosity is treated as a tensor, unlike eddy viscosity. An overall agreement of the obtained results with the existing literature for the jet flow proves the effectiveness of the new closure equations. Besides, turbulent stresses as a function of normalized mean velocity are found to exhibit their odd and even symmetries, which seem to be the manifestations of the free energy symmetry of continuous phase transition.

Keywords: phase transition, free energy, order parameter, symmetry, closure equation, viscosity tensor.

1. Introduction

Turbulent flow is characterized by a hierarchy of scales of fluctuations ranging from production to dissipation. The dynamics of turbulent flow is governed by the Navier-Stokes equations, whose solution resolving all those scales at high Reynolds number in complex geometries is unlikely to be attainable in the foreseeable future. However, Reynolds averaging and filtering are the two methods that have been used to transform the Navier-Stokes equations so that the small-scale turbulent fluctuations do not have to be directly simulated. Both methods introduce additional terms in the governing equations due to the correlations of fluctuating quantities (i.e., turbulent stresses) that need to be modeled in order to achieve closure. The closure assures a sufficient number of equations for all the unknowns. Turbulence modeling requires that turbulent stresses in the Reynolds averaged Navier-Stokes (RANS) equations be appropriately modeled¹. Boussinesq hypothesis² is the core of all turbulence models that relates the Reynolds stresses to the mean velocity gradients as

$$-\overline{u'_i u'_j} = \nu_T \left(\partial \bar{u}_i / \partial x_j + \partial \bar{u}_j / \partial x_i \right) \quad (1)$$

for incompressible fluid which is analogous to the laminar one with enlarged viscosity called the eddy viscosity. This eddy viscosity requires further modeling as, for example, $\nu_T = \ell_m^2 \left(\partial \bar{u} / \partial y \right)$ after Prandtl³,

$\nu_T = C_\mu \ell_m \sqrt{k}$ after Kolmogorov⁴ and Prandtl⁵,

$\nu_T = C_\mu k^2 / \varepsilon$ after Launder and Spalding⁶, where ℓ_m is the mixing length (closely related to the length scale).

Present endeavor aims at extracting turbulence closure equations by using the features of continuous (also called second-order) phase transition against the order parameter. The concept of order parameter in

phase transition has been widely generalized as when an arbitrary system crosses an instability point, only a few variables become relevant and serves as an order parameter, which may be single or coupled variables that distinguishes the ordered from the disordered phase. However, the averaged velocity may be a suitable control parameter for a fluid dynamical system which if adequately tuned, the system can undergo strong qualitative changes in its macroscopic properties and consequently in microscopic properties. Goldenfeld⁷ showed that the rise of temperature in metals is similar to the increase in velocity in the fluid flows, the former causes magnetization at critical point and the latter turbulence. This invokes a strong analogy between turbulization and magnetization at critical point⁷⁻⁹. Recently, many researchers have demonstrated both experimentally and numerically by resolving the time and length scales sufficiently close to the critical point that all turbulent flows are closely analogous to the continuous phase transition (CPT)¹⁰⁻¹³. In CPT, Landau-free energy¹⁴ of a system exhibits symmetry against the order parameter. This free energy of the system and the kinetic energy of turbulence are analogous because both near their critical points obey the power-law scaling of the correlation functions¹⁵.

2. Closure equations due to phase transition

Navier-Stokes equations represent the collective motion of fluid particles. These equations of motion for incompressible fluid are

$$\frac{\partial \bar{u}_i}{\partial t} + \bar{u}_j \frac{\partial \bar{u}_i}{\partial x_j} = -\frac{\partial}{\partial x_j} \left(\frac{\bar{p}}{\rho} \delta_{ij} + \overline{u'_i u'_j} \right) + \nu \frac{\partial^2 \bar{u}_i}{\partial x_j^2}. \quad (2)$$

In collective motion, the most naturally (but not necessarily) chosen order parameter is the predominant velocity¹⁶. The concept of moving equilibrium¹⁷ states

that the rate of change of each component of Reynolds stress $\overline{u'_i u'_j}$ is proportional to the rate of change of turbulence kinetic energy k , that is, $\overline{u'_i u'_j}$ corresponds to the free energy of phase transition.

In view of relating the features of phase transition to the dynamics of turbulence, an implicit function $f(\overline{u_i}, \overline{u'_i u'_j}) = 0$ for RANS equation (2) is written as

$$f(\overline{u_i}, \overline{u'_i u'_j}) = \frac{d\overline{u_i}}{dt} + \frac{\partial}{\partial x_j} \left(\frac{\overline{p}}{\rho} \delta_{ij} + \overline{u'_i u'_j} \right) - \nu \frac{\partial^2 \overline{u_i}}{\partial x_j^2}. \quad (3)$$

The differential form of the implicit function is $(\partial f / \partial \overline{u_i}) d\overline{u_i} + (\partial f / \partial \overline{u'_i u'_j}) d\overline{u'_i u'_j} = 0$. At the point of phase transition, the fluctuation correlations $\overline{u'_i u'_j}$

become maximum, that is, $\overline{d\overline{u'_i u'_j}}$ become zero leading to $\partial f / \partial \overline{u_i} = 0$ because $d\overline{u_i}(x_j) = 0$ is unrealistic.

Equation $\partial f / \partial \overline{u_i} = 0$ is the first derivative of the free energy (RANS equation) with respect to the order parameter $\overline{u_i}$ that expresses the state of turbulence in terms of free energy equilibrium and thus combines the dynamics of turbulence with that of CPT as

$$\frac{\partial}{\partial \overline{u_i}} \frac{\partial}{\partial x_j} \left(\frac{\overline{p}}{\rho} \delta_{ij} + \overline{u'_i u'_j} \right) = 0. \quad (4)$$

This equation can be written by using an entity $f_I(\overline{u_i}) \partial \overline{u_j} / \partial x_j = 0$ due to the continuity equation as

$$\frac{\partial}{\partial \overline{u_i}} \frac{\partial}{\partial x_j} \left(\frac{\overline{p}}{\rho} \delta_{ij} + \overline{u'_i u'_j} \right) = f_I(\overline{u_i}) \frac{\partial \overline{u_j}}{\partial x_j} \quad (5)$$

which, upon integration yields

$$\overline{u'_i u'_j} = -\frac{\overline{p}}{\rho} \delta_{ij} + \iint f_I(\overline{u_i}) d\overline{u_i} d\overline{u_j}. \quad (6)$$

Let the free energy of turbulence be defined as

$$F_{ij} = \overline{u'_i u'_j} - b_n \overline{u^{(i)} u^{(j)}} (\overline{u} / u_c) \delta_{ij} \quad (7)$$

where the first term on the right-hand side is the energy that enters into the turbulence by the interaction of fluctuations and mean field shear, and the second term is the energy that leaves the turbulence due to the

coupling between turbulent fluctuations and order parameter, and all these energies finally dissipate as heat. The indices (i) and (j) in the parentheses indicate that they are not summed over. Here \overline{u} -velocity is the order parameter being the predominant one and normalized by centerline velocity u_c , and b_n is a constant to accommodate the effect of normalization of the order parameter. Landau-free energy is a thermodynamic potential of a system despite being expressed as a function of the order parameter and its conjugate external field. Turbulence-free energy in Eq. (7) is a close analog to the thermodynamic potential form of Landau-free energy.

On replacing $\overline{u'_i u'_j}$ by $\overline{u'_i u'_j} - B_{(i)} \overline{u}^2 (\overline{u} / u_c) \delta_{ij}$, Eq. (6) becomes

$$\overline{u'_i u'_j} = \left(B_{(i)} \overline{u}^3 / u_c - \frac{\overline{p}}{\rho} \right) \delta_{ij} + \iint f_I(\overline{u_i}) d\overline{u_i} d\overline{u_j} \quad (8)$$

where B_i is a constant tensor and $\overline{u^{(i)} u^{(j)}}$ is replaced by \overline{u}^2 using order of magnitude reasoning. Equation (8) may be written further as

$$\overline{u'_i u'_j} = C_{(i)(j)} \left(\left(B_{(i)} \overline{u}^3 / u_c - \frac{\overline{p}}{\rho} \right) \delta_{ij} + \iint f_I(\overline{u_i}) d\overline{u_i} d\overline{u_j} \right) \quad (9)$$

where C_{ij} are the scaling constants for a balance between the turbulent and the mean quantities of the equation, and the function $f_I(\overline{u_i})$ is ascertained later.

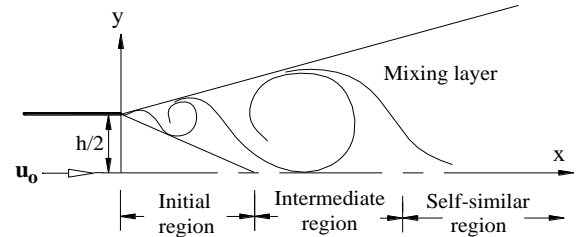


Fig. 1 Schematic of a plane turbulent jet.

3. Application to a plane jet flow

The derived closure equations are applied to unclosed RANS equations for a plane jet as a test case.

Plane jets are free shear flows where fluids coming out from a two-dimensional (2D) orifice mix with the ambient fluid and develop through three successive distinct regions, namely initial, intermediate, and developed regions (Fig. 1). Initial region (at $x/h \leq 6$) is characterized by the presence of a potential core of uniform axial velocity that is in laminar state, intermediate region by the transition state and developed region by the turbulent state. Literature¹⁸ shows a large scatter of the downstream distance at which the jet becomes fully developed, ranging from $5h$ to $25h$, depending on its initial conditions (e.g., Reynolds number at exit and nozzle geometry). This jet grows non-linearly in the developing (initial and intermediate) region and linearly in the developed (self-similar) region. The governing equations and their initial and boundary conditions, determination of the constants C_{ij} and function $f_I(\bar{u}_i)$, the closure equations in (x, y, z) coordinates, and description of the plotting of turbulent stresses are presented in this section.

3.1 Governing equations

Continuity and RANS equations describing a steady plane turbulent jet flow for incompressible fluid are

$$\frac{\partial \bar{u}_i}{\partial x_i} = 0 \quad (10)$$

$$\bar{u}_j \frac{\partial \bar{u}_i}{\partial x_j} = -\frac{1}{\rho} \frac{\partial \bar{p}}{\partial x_i} + \frac{\partial}{\partial x_j} \left(\nu \frac{\partial \bar{u}_i}{\partial x_j} - \overline{u'_i u'_j} \right) \quad (11)$$

where $-\overline{u'_i u'_j} = \nu_{T(i)(j)} (\partial \bar{u}_i / \partial x_j + \partial \bar{u}_j / \partial x_i)$ is the turbulent stress and strain rate relation and $\nu_{T,ij}$ the

turbulent viscosity tensor. Equations (9)-(11) are in closed form and need to be solved to extract mean and turbulence quantities of the flow.

3.2 Initial and boundary conditions

In free jet flow, the initial conditions are $\bar{u}(0, y \leq 0.5h) = u_o$, $\bar{u}(0, y > 0.5h) = 0$ and $\bar{v}(0, y) = 0$ where h is the orifice height and u_o the uniform jet exit velocity. The boundary conditions are: ϕ (general flow variable) attains ambient conditions at the jet outer edge, $\partial \phi / \partial x = 0$ at the outflow, and $\partial \phi / \partial y = 0$ at the symmetry axis except $\bar{v} = 0$ and $\overline{u'v'} = 0$.

3.3 Determination of C_{ij}

The concept of moving equilibrium¹⁷ may be read in explicit form as

$$\overline{u'_i u'_j} = a_{(i)(j)} (\delta_{ij} \pm \varepsilon_{ijk}) k \quad (12)$$

where a_{ij} are the proportionality constants. From Eqs. (9) and (12), one can write

$$\begin{aligned} \overline{u'_i u'_j} \sim & \left(B_{(i)} \bar{u}^3 / u_c - \frac{\bar{p}}{\rho} \right) \delta_{ij} \\ & + \iint f_I(\bar{u}_i) d\bar{u}_i d\bar{u}_j \sim (\delta_{ij} \pm \varepsilon_{ijk}) k. \end{aligned} \quad (13)$$

This equation indicates that C_{ij} of Eq. (9) and a_{ij} of Eq. (12) are structurally similar, and hence $a_{ij} = C_o C_{ij}$ for

C_o is a constant. Using $\overline{u'v'} / \sqrt{\overline{u'u'}} \sqrt{\overline{v'v'}} \approx 0.46$ and $\overline{u'v'} / k \approx 0.35$ for turbulent flows and $\overline{u'u'} \approx 1.4 \overline{v'v'}$ for plane jet flow¹⁹ along with Eq. (12), the constants are evaluated to be $a_{11} = 0.87$, $a_{22} = 0.62$ and $a_{12} = 0.35$. The values of C_{ij} are calculated later by knowing the value of C_o .

3.4 $f_I(\bar{u}_i)$ and closure equations in (x, y, z)

The free energy of turbulence $\overline{u'_i u'_j}$ may be expressed by a fourth degree polynomial of normalized velocity \bar{u}/u_c with a view to capture the free energy symmetry of continuous phase transition. Analysis of turbulent shear stress data of plane and circular jets²⁰⁻²¹ show that the coefficient of the fourth-order term is insignificant compared to other coefficients of that polynomial in the initial region of the jet while the same is more significant than or comparable to other coefficients in the intermediate and self-similar regions. Furthermore, the coefficients of the second-order term of the polynomials higher than the fourth degree are found small, which is inconsistent with the order of magnitude estimate of $\overline{u'v'}$ by dimensional analysis. It seems now that $\overline{u'v'}$ is best expressed by a third degree polynomial of \bar{u}/u_c in the initial region of the jet and by a fourth degree polynomial beyond the initial region. Such a polynomial may be assumed as $-\overline{u'v'}/u_c^2 = c_s (U - U^2 + U^3 - U^4)$ for the turbulent shear stress. This shear stress is generally symmetric with respect to the origin (called odd symmetric) while the normal stresses are symmetric with respect to the axis (called even symmetric). Hence, turbulent normal stress function may be obtained by integrating the above polynomial as

$$\overline{u'u'}/u_c^2 = C_n U \left(U - \frac{1}{2}U + \frac{1}{3}U^2 - \frac{1}{4}U^3 + \frac{1}{5}U^4 + \text{rest} \right),$$

which further can be approximated as

$$\overline{u'u'}/u_c^2 = C_n U \exp(-\alpha U) \text{ where } U = \bar{u}/u_c, \text{ and } C_s, C_n$$

and α are constants. This is because an odd symmetric function, either by differentiation once or by integration, becomes even symmetric and vice-versa.

The function $f_l(\bar{u})$ for the Reynolds stresses is obtained from Eq. (5), discarding the pressure term by using their functional form for the normal stress and by using the highest order term of the polynomial for the shear stress. The derived function $f_l(\bar{u})$ for the axial normal stress $\overline{u'u'}$ is $f_u(\bar{u}) = \partial^2(\overline{u'u'})/\partial u \partial u$, i.e.

$$f_u(\bar{u}) = C_n u_c \beta (-2 + \beta \bar{u}) \exp(-\beta \bar{u}) \quad (14a)$$

where $\beta = \alpha/u_c$, for the transverse normal stress $\overline{v'v'}$

is $f_v(\bar{u}) = \partial^2(\overline{v'v'})/\partial v \partial v$, i.e.

$$f_v(\bar{u}) = (a_{22}/a_{11}) (\partial \bar{u} / \partial v)^2 f_u(\bar{u}) \quad (14b)$$

and for the shear stress $\overline{u'v'}$ is

$$f_s(\bar{u}) = \partial^2(\overline{u'v'})/\partial u \partial v. \quad (14c)$$

That is $f_s(\bar{u}) = C_s \bar{u}/u_c$ for the initial region of the jet

and $f_s(\bar{u}) = C_s \bar{u}^2/u_c^2$ beyond the initial region. The

highest order term is used instead of the entire polynomial for the shear stress as this requires known values of the coefficients that might cause ascertaining

$f_s(\bar{u})$ unlikely. Further, the function $f_s(\bar{u})$ is the

second derivative of the highest order term of the polynomial, as a result, retains the same characteristics of

$f_s(\bar{u})$ if were obtained by using the entire polynomial.

Above reasons justify the use of the highest order term instead of the entire polynomial to determine $f_s(\bar{u})$.

Using the functions $f_u(\bar{u})$, $f_v(\bar{u})$ and $f_s(\bar{u})$, closure equation (9) in (x, y, z) coordinates becomes

$$\overline{u'u'} = C_{11} \left(B_1 \bar{u}^{-3}/u_c - \frac{\bar{p}}{\rho} + \iint f_u(\bar{u}) d\bar{u} d\bar{u} \right) \quad (15a)$$

$$\overline{v'v'} = c_{22} \left(B_2 \bar{u}^{-3}/u_c - \frac{\bar{p}}{\rho} + \frac{c_{22}}{c_{11}} \iint f_u(\bar{u}) d\bar{u} d\bar{u} \right) \quad (15b)$$

$$\overline{u'v'} = C_{12} \iint f_s(\bar{u}) d\bar{u} d\bar{v}. \quad (15c)$$

3.5 Plotting of Reynolds stresses

Equation (15a) is in the velocity domain and, by simplifying, may be reduced to

$$\overline{u'u'^u} = \iint f_u(\bar{u}) d\bar{u} d\bar{u} \quad (16)$$

which may also be written in the space domain as

$$\overline{u'u'^y} = \iint f_u(\bar{u}) \left(\frac{\partial \bar{u}}{\partial y} \right)^2 dy dy. \quad (17)$$

It can be shown that $\overline{u'u'^y} = \beta \overline{u'u'^u}$ for β is a constant

greater than unity. The graphs of $\overline{u'u'^u}$ and $\overline{u'u'^y}$ against y-axis are not equal in area because of the difference in integration limits across the stream between the outer edge and centerline of the jet. In the former case, the limits cover the entire velocity domain and in the latter case, they cover half of the space

domain. Now, $\int \overline{u'u'^u} dy' = \int \overline{u'u'^y} dy$ where $y' = \lambda y$

for λ is a constant, and this relation leads to $\beta = \lambda$.

Hence, Reynolds stresses due to Eqs. (15) must be

plotted as $\beta \overline{u'u'^u}$ against λy .

4. Numerical strategies

A CFD (Computational Fluid Dynamics) code is developed for solving 2D steady flow based on finite volume method and rectangular structured grid²². SIMPLE (Semi-Implicit Method for Pressure Linked Equations) algorithm of Patankar and Spalding²³ is employed to solve the equations (9)-(11) governing the plane turbulent free jet. Discretization of the governing equations, computational grids, and grid convergence test are described in this section.

4.1 Discretization and computational grids

The convective and diffusive terms of the transport equations for ϕ are discretized using the second-order upwind difference scheme and the second-order central difference scheme in the staggered grid, respectively, with cell centers for \bar{u} at (i, J) , for \bar{v} at (I, j) , for \bar{p} , $\overline{u'u'}$ and $\overline{v'v'}$ at (I, J) , and for $\overline{u'v'}$ at (i, j) . The discretized equations are solved iteratively using the line-by-line tridiagonal matrix algorithm²⁴ (TDMA). The momentum and pressure correction equations are provided with a suitable number of sweeps. All variables $(\bar{u}, \bar{v}, \bar{p})$ are weighted with very low under-relaxation factors (order of 0.1) for the stability of the numerical scheme. The flow variables are further expressed by a weighted average of their neighbors in

each iteration after obtaining them using TDMA. This procedure ensures the stability of the numerical scheme by reducing the oscillations of strain rates in turbulent viscosity calculation from the stress and strain rate relation.

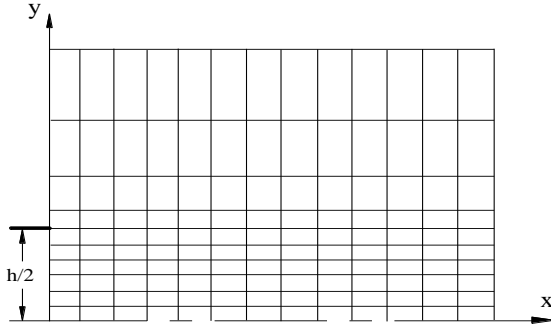


Fig. 2 Computational grids for a plane turbulent jet.

The flow domain is constructed over $40h \times 20h$ in xy -directions with grids as in Fig. 2. Grids are uniform inside the orifice and varying outside it in y -direction, and uniform in x -direction as in the figure. The solutions are duly converged with the normalized residuals of 1.2×10^{-6} , 6.0×10^{-6} and 6.4×10^{-5} for \bar{u} , \bar{v} and mass, respectively.

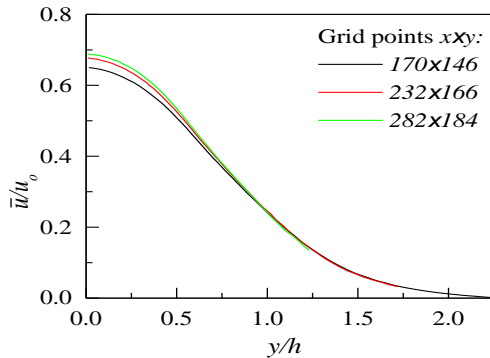


Fig. 3 Axial mean velocity profiles at $x/h=5$.

4.2 Grid convergence test

The present simulation is performed for a plane turbulent free jet with Reynolds number $Re=3.2 \times 10^4$, orifice height $h=0.04m$, and velocity at exit $u_0=12 m/s$. A grid convergence test is carried out with the three grid sizes termed coarse, medium and fine which are 170×146 , 232×166 and 282×184 in xy -directions having a grid refinement factor of 1.45 between the

coarse and fine grids. Figure 3 depicts the mean axial velocity profiles at $x/h=5$ for the three grid sets. Grid refinement shows successful convergence for those three grid resolutions. The results presented here are obtained by using the fine mesh.

5. Results and discussion

Closed form RANS equations (9)-(11), governing the turbulent flow, are solved numerically for a plane jet. The used numerical scheme is found to produce stable solutions for $B_1=2.4$ and $B_2=1.8$, and for $C_{11}=0.048$, $C_{22}=0.034$ and $C_{12}=0.019$ that are obtained by using the relation $C_{ij} = a_{ij}/C_o$ for a minimum value of $C_o \approx 18.2$. Values of other constants appearing in the functions $f_1(\bar{u})$ for turbulent shear and normal stresses from the stable numerical scheme are $C_s=320$, $C_n=5.8$ and $\alpha=3$ in the initial region of the jet and $C_s=240$, $C_n=7.4$ and $\alpha=2$ beyond the initial region. This section presents axial velocity, transverse velocity, and turbulent stresses that are extracted in the present simulation and their comparison with the existing theoretical¹⁸, experimental (Exp), and numerical data on planar turbulent jets. Klein *et al.*¹⁹ performed direct numerical simulation (DNS) of a turbulent plane jet with $Re=4 \times 10^3$ and compared their results (e.g., mean velocity and Reynolds stresses) with the results of several authors and found them in good agreement. Heschl *et al.*²⁰ made RANS simulation of a plane jet with $Re=3 \times 10^4$ using the standard $k-\epsilon$ turbulence model and compared their results with the existing data. Ramaprian and Chandrasekhara²⁵ with $Re=1.6 \times 10^3$ have experimentally investigated the plane jets and presented the profiles of mean velocity and turbulent stresses.

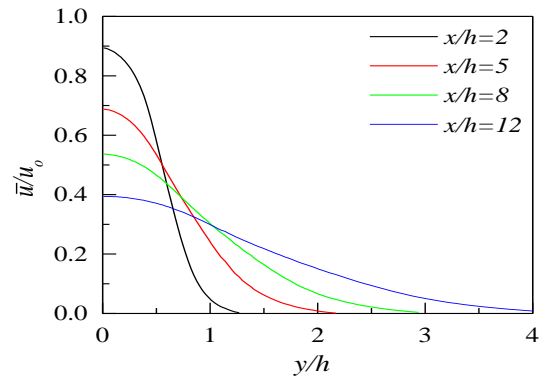


Fig. 4 Axial mean velocity profiles.

Mean axial velocity \bar{u}/u_o is presented in Fig. 4 against the transverse distance y/h at axial locations $x/h=2, 5, 8$ and 12 . This figure illustrates that the jet grows with the axial distance due to the entrainment of ambient fluid, and its maximum velocity decreases due to the loss of momentum caused by the interaction with the ambient fluid. Figure 5 presents normalized mean velocity \bar{u}/u_c against $y/y_{1/2}$ at axial location $x/h=12$ along with Gaussian curve¹⁸ of the form $\bar{u}/u_c = \exp(-0.693\eta^2)$ and DNS results¹⁹ where $\eta=y/y_{1/2}$, and $y_{1/2}$ is the jet's half-width. The figure shows that results from the present simulation and DNS compare well with the Gaussian curve. Transverse

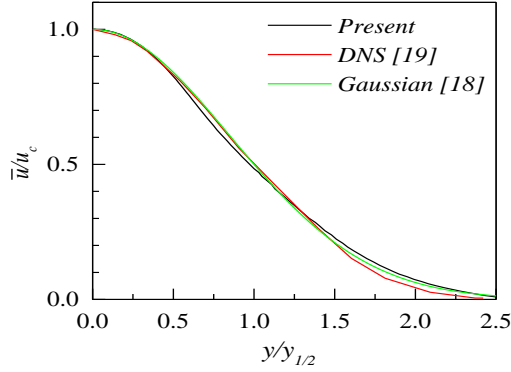


Fig. 5 Axial mean velocity at $x/h=12$.

velocity \bar{v}/u_c is depicted in Fig. 6 against $y/y_{1/2}$ at axial locations $x/h=8$ and 12 , and found to have achieved free-stream value at some larger distance $y/y_{1/2} > 3.5$ (not shown). DNS¹⁹ and experimental²⁵ data for \bar{v} -velocity provided in the figure are in satisfactory agreement with the present simulation.

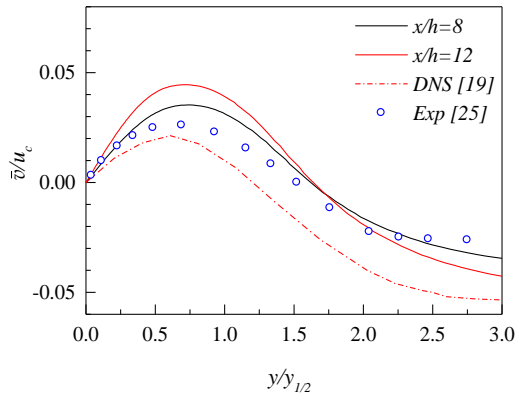


Fig. 6 Transverse mean velocity profiles.

Reynolds normal stresses $\overline{u'u'}/u_c^2$ and $\overline{v'v'}/u_c^2$, and shear stress $\overline{u'v'}/u_c^2$ are calculated from Eq. (15) and plotted in Figs. 7-9 against $y/y_{1/2}$ at $x/h=8$ and 12 for $\lambda \approx 1.5$ (a constant appeared in Sec. 3.5). Calculated stresses from DNS¹⁹, RANS simulation²⁰ and measurements²⁵ are added to compare in those figures. All turbulent stresses, $\overline{u'u'}$, $\overline{v'v'}$ and $\overline{u'v'}$ from the present simulation, are observed in close agreement with the stresses from measurement and simulations.

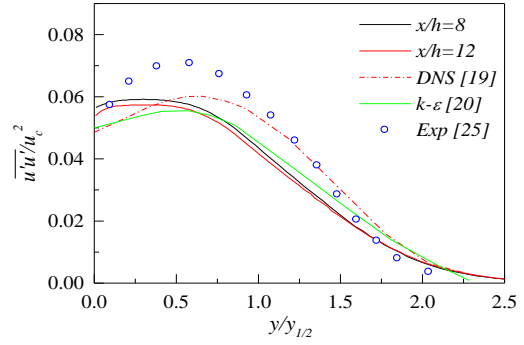


Fig 7. Axial normal stress profiles.

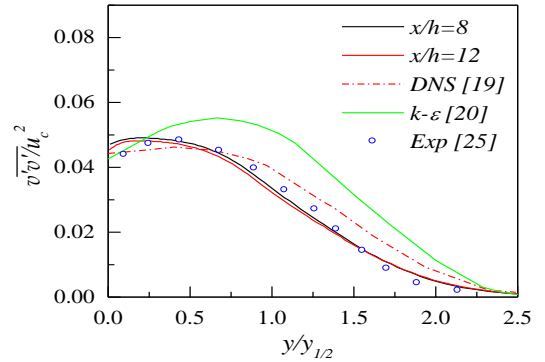


Fig. 8 Transverse normal stress profiles.

6. Conclusions

The new closure equations derived by considering turbulence as CPT are utilized here to get the closed form RANS equations. The numerical solution of those equations for a plane jet flow provides the mean axial and transverse velocities, and turbulent stresses. Extracted results from the simulation are found to be in overall agreement with the existing data, showing the effectiveness of the closure equations. Turbulent stresses of the jet as functions of normalized mean axial velocity confirm their odd and even symmetries, and

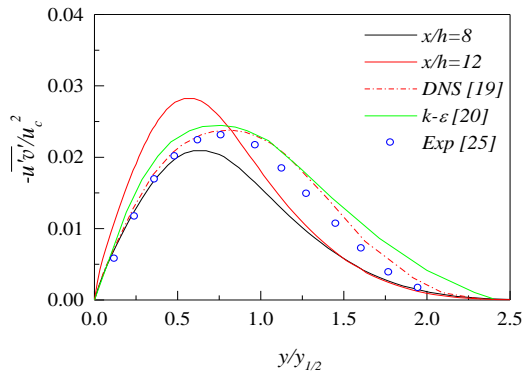


Fig. 9 Reynolds shear stress profiles.

owning of the additional term like the one in Landau-free energy expansion¹⁴, and thus demonstrate the phenomenological relations with phase transition and restate that laminar-turbulent transition undergoes a continuous phase transition.

References

- ¹O. Reynolds, On the dynamical theory of incompressible viscous fluids and determination of the criterion, *Phil. Trans. Roy. Soc. A* 186, 123 (1895).
- ²J. Boussinesq, *Theorie de l'ecoulement tourbillant*, *Mem. Pres. Acad. Sci.* 23, 46 (1877).
- ³L. Prandtl, Über die ausgebildete turbulenz, *ZAMM* 5, 136 (1925).
- ⁴A.N. Kolmogorov, Equations of turbulent motion of an incompressible fluid, *Izv. Acad. Nauk USSR, Ser. Fiz.* 6, 56 (1942).
- ⁵L. Prandtl, Über ein neues formelsystem für die ausgebildete turbulenz, *Nachr. Akad. Wiss. Göttingen, Math.-Phys.Kl.*, 6 (1945).
- ⁶B.E. Launder and D.B. Spalding, *Mathematical Models of Turbulence* (Academic Press, London, 1972).
- ⁷N. Goldenfeld, Roughness induced critical phenomena in a turbulent flow, *Phys. Rev. Lett.* 96, 044503 (2006).
- ⁸S.T. Bramwell, P.C. W. Holdsworth, and J.-F. Pinton, Universality of rare fluctuations in turbulence and critical phenomena, *Nature* 396, 552 (1998).
- ⁹Ch. Chatelain, P.E. Berche and B. Berche, Second-order phase transition induced by deterministic fluctuations in aperiodic eight-state Potts models, *Eur. Phys. J. B* 7, 439 (1999).

- ¹⁰W.S. Gan, Application of spontaneous broken symmetry to turbulence, *Proc. ICSV16, Krakow, Poland* (2009).
- ¹¹K. Avila, D. Moxey, A. de Lozar, M. Avila, D. Barkley and B. Hof, The onset of turbulence in pipe flow, *Science* 333, 192 (2011).
- ¹²N. Vladimirova, S. Derevyanko, and G. Falkovich, Phase transitions in wave turbulence, *Phys. Rev. E* 85, 010101 (2012).
- ¹³L. Shi, G. Lemoult, K. Avila, S. Jalikop, M. Avila and B. Hof, The universality class of the transition to turbulence, *arXiv:1504.03304, physics.flu-dyn* (2015).
- ¹⁴P. C. Hohenberg and A. P. Krekhov, An introduction to the Ginzburg-Landau theory of phase transitions and nonequilibrium patterns, *arXiv:1410.7285, cond-mat* (2015).
- ¹⁵N. Goldenfeld and H.-Y. Shih, Turbulence as a problem in non-equilibrium statistical mechanics, *J. Stat. Phys.* 167, 575 (2017).
- ¹⁶T. Vicsek and A. Zafeiris, Collective motion, *Phys. Reports* 517, 71 (2012).
- ¹⁷P.A. Durbin and B.A.P. Reif, *Statistical Theory and Modeling for Turbulent Flows* (John Wiley and Sons, 2011).
- ¹⁸R.C. Deo, J. Mi and G.J. Nathan, The influence of Reynolds number on a plane jet, *Phys. Fluids* 20, 075108 (2008).
- ¹⁹M. Klein, A. Sadiki and J. Janicka, Investigation of the influence of the Reynolds number on a plane jet using direct numerical simulation, *Int. J. Heat and Fluid Flow* 24, 785 (2003).
- ²⁰C. Heschl, K. Inthavong, W. Sanz and J. Tu, Evaluation and improvements of RANS turbulence models for linear diffuser flows, *Computers & Fluids* 71, 272 (2013).
- ²¹H. Fellouah, C.G. Ball and A. Pollard, Reynolds number effects within the development region of a turbulent round free jet, *Int. J. Heat and Mass Transfer* 52, 3943 (2009).
- ²²M.A. Azim, Numerical study of closely spaced twin circular jets, *Int. J. Fluid Mech. Res.* 47, 407 (2020).
- ²³S.V. Patankar and D.B. Spalding, A calculation procedure for heat, mass and momentum transfer in three dimensional parabolic flows, *Int. J. Heat Mass Transfer* 15, 1787 (1972).
- ²⁴L.H. Thomas, Elliptic problems in linear difference equations over a network, *Watson Sci. Comput. Lab. Report*, Columbia University, New York (1949).
- ²⁵B.R. Ramaprian and M.S. Chandrasekhara, LDA measurements in plane turbulent jets, *ASME J. Fluids Eng.* 107, 264 (1985).

Comments: a) Revision of implicit function and turbulence-free energy in Sec. 2 cause minor changes in the results. b) Revision of Eq. (14c) in Sec. 3.4 does not affect the results. c) Revision in Sec. 3.5 provides more clarity.